A Remotely Central Dimming System for a Large-Scale LED Lighting Network Providing High Quality Voltage and Current

Radwa M. Abdalaal, *Student Member, IEEE,* Carl Ngai Man Ho, *Senior Member, IEEE,* Carson K. Leung, *Senior Member, IEEE*, and Henry S. H. Chung, *Fellow, IEEE*

***Abstract* -- Standard TRIAC-based dimmers introduce power quality issues especially for a large-scale lighting network. Other existing dimming protocols involve additional wiring systems and/or additional controllers to LED drivers. This paper proposes a central dimming system for a large penetration of Light Emitting Diode (LED) lamps. The dimming system is remotely control through a webpage or a desktop application. Dimming is achieved while maintaining high voltage and current quality waveforms, which results in a high power factor and a low input current harmonic distortion. The system does not require additional wiring nor specific adjustments to commercial dimmable LED drivers. The system allows scheduling a dimming profile to endorse energy saving. In the proposed dimming system, dimming function is achieved by connecting a voltage source converter (VSC) between the grid and the LED lamps. An advanced feature is added to the VSC dimmer to remotely send/receive messages between the system and the user through a Graphical User Interface. Thus, the user can communicate with the VSC dimmer by sending commands and receiving feedback information. The influence of communication delay on system stability is analyzed by using small signal models. A VSC dimmer prototype (500VA/120V) has been built with a communication module to provide remote control. Experimental results and comparisons between utilizing the TRIAC-based dimmer and the VSC dimmer for dimming function are discussed in the paper.**

***Index Terms*— Dimmer, LED, power quality, Remote Dimming, TRIAC, VSC.**

I. INTRODUCTION

TECHNOLOGICAL advancement of Light Emitting Diode (LED) offers 1) long lifetime, 2) high luminous efficacy 3) environmentally friendly 4) high color rendering index greater than 95 [2]. LEDs are now utilized for different indoor and outdoor lighting applications. A dimming function is required to regulate the light intensity to achieve energy saving, aesthetic pleasure, and increase productivity. Dimming can also expand the lifetime of an LED [3]. An LED dimming system consists of an LED string, as the light source, an LED driver and a dimmer. A dimmer, sometimes referred to as a controller, is usually placed between the main supply and the LED driver. The LED driver can either sense the changes in the input voltage or receive an external dimming signal according to the dimming protocol implemented. Based on this information, the driver adjusts its forward current in response to its dimming operation. Utilizing different dimming protocols has brought concerns to their impact on the power quality (PQ) of the network. Even though an LED bulb shows a good PQ parameters under rated operating point [4], its current harmonic distortion level under different dimming intensities might violate the standard values depicted by IEC61000-3-2 [5]. Despite the low power consumption of individual bulbs, a high penetration of LEDs connected to the same feeder would pollute the network at distribution levels [6]. The IEEE standards PAR1789 highlight that existing LED drivers' technologies may provoke potential health risks due to visible and invisible flickering [7]. Several research work are being developed to improve LED drivers that provide precise dimming control [8], [9]. Various power quality tests have been applied on commercial dimmable LED lamps in [10]. It was found that for dimmable LEDs, the output light intensity of the lamp is sensitive to voltage variations in the network. This causes a visible light flickering to a human eye. Dimming of a ballast driven lighting system to achieve high PQ is proposed in [11], by connecting a reactive power device in series between the grid and the ballast. This method is appropriate for inductive high-intensity discharge (HID) lamps, and not compatible with LEDs.

A new remote controlled dimming system, while improving PQ parameters, is proposed in this paper. The system can provide the following features,

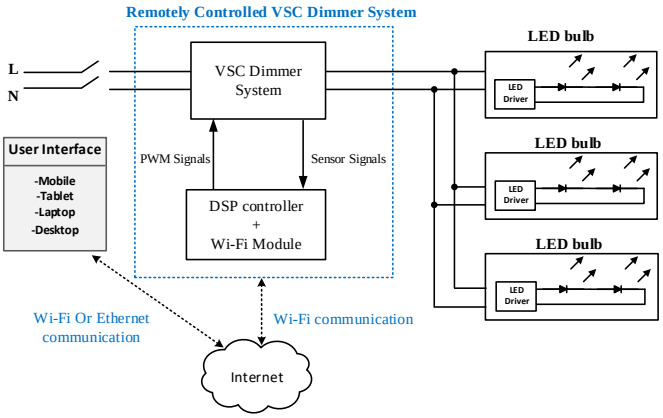

Fig. 1. Proposed remote control VSC dimmer system.

Manuscript received Month xx, 2019; revised Month xx, 2019; accepted Month x, 2019. This is an updated version of conference paper [1]. This work was supported in part by a grant from the Canada Research Chairs, Canada (Sponsor ID: 950-230361).

R.M. Abdalaal, and C.N.M. Ho (Corresponding author) are with Dept. of Electrical & Computer Engineering, University of Manitoba, Winnipeg, MB, Canada (e-mail: abdalaal@myumanitoba.ca; carl.ho@umanitoba.ca).

C. K. Leung is with Dept. of Computer Science, University of Manitoba, R3T5V6, Winnipeg, MB, Canada (e-mail: kleung@cs.umanitoba.ca).

H. S. H. Chung is with Dept. of Electronic Engineering, City University of Hong Kong, Hong Kong SAR, China (e-mail: eeshc@cityu.edu.hk).

1) One central dimmer can serve a large number of LED lamps.
2) No rewiring for existing lighting network and low-cost commercial dimmable LED lamps can be used.
3) Achieving high current and voltage quality with a wide range of LED dimming.
4) Able to compensate most of static and dynamic voltage variations in the network.
5) Remote control dimming and monitoring with capability to schedule a dimming profile.

The proposed dimming system is compatible with dimmable commercial LEDs. Non-dimmable LEDs in the market cannot be dimmed using this technique. The system employs connecting a Voltage Source Converter (VSC) system between the grid and the lighting network as shown in Fig. 1. In order to differentiate the proposed system and existing solutions, a review of existing dimmer technologies, along with the pros and cons including phase cut, analog, digital, and wireless dimming protocol is presented.

II. State of Art of Dimming Technology

Existing work in the literature review and the market includes wired and wireless dimming systems. It should be noted that the dimmable LED driver has to be compatible with the dimming method used.

A. LED Driver Dimming Techniques

Amplitude Modulation (AM) and Pulse Width Modulation (PWM) techniques are two common dimming techniques that are employed in an LED driver to achieve LEDs illuminance control. As the light intensity is proportional to the LED current flow [12], both techniques are controlling the average current going through the LED string. In AM technique, also called continuous current reduction (CCR), dimming is achieved by controlling the magnitude of the forward DC current fed to the LED string as shown in Fig. 2 (a). Under PWM technique, the diode string is turned on and off completely with a fixed frequency. During the on state, the LED current will reach its rated value as illustrated in Fig. 2 (b). By varying the duty cycle (d) the average forward current will be changed. The output light intensity will be proportional to the duty cycle as,

$$I_{Favg} = I_F * d \quad (1)$$

where, I_{Favg} is average forward diode current and I_F is maximum forward current of the LED string.

AM is simple to implement as it does not require additional electronic circuit connection. However, variation of LED current may cause color temperature change of the emitted light [13]. On the other hand, PWM technique drives the LED string at the rated forward current provided by the manufacturer, preventing color temperature change. PWM technique also provides good regulation at very low current levels. The frequency of the PWM should be high enough to avoid flickering. Fast transients of simultaneous switching of LEDs might cause electromagnetic interference (EMI) and potential noise could be generated [14], [15]. Hybrid AM/PWM dimming technique to combine the advantages of both techniques is also proposed in the literature [16], [17].

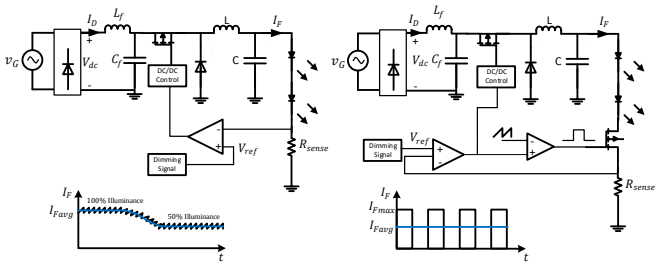

(a) (b)

Fig. 2. Dimming techniques (a) AM (b) PWM.

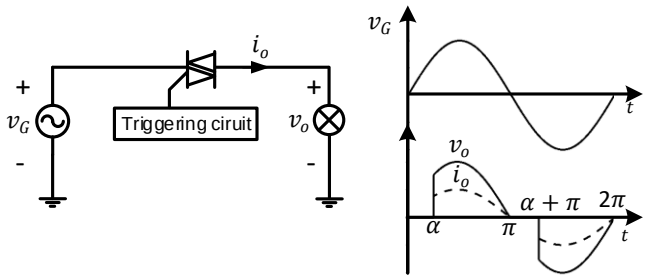

(a) (b)

Fig. 3. Standard TRIAC-dimmer lighting system.

B. TRIAC-Based Dimmers

Existing phase cut dimmer system includes a standard TRIAC-based dimmer with a triggering circuit, as shown in Fig. 3 (a). The power sent to the bulb is controlled by controlling the phase angle delay α, which results in an adjustable light illuminance. Nevertheless, for a desired dimming level the delay angle is not zero. Consequently, there will be a deviation of the input current from its sinusoidal shape. Typical waveforms of a TRIAC dimmer circuit for a resistive load is shown in Fig. 3 (b). The compatibility of LED lamps with standard TRIAC dimmers has brought many challenges. The low input current absorbed by an LED, which could be lower than the TRIAC holding current, results in a restricted dimming profile range. The LED lamp current has to be sufficient enough otherwise the user might experience light flickering. In order to overcome these challenges, a phase angle detection circuit and a passive, active or adaptive bleeder is utilized to adjust the LED current and maintain the latching and holding current of the TRIAC dimmer [18]. An addition bleeder circuit will add cost and increase losses of the overall system. Generally, employing a TRIAC dimmer is cost effective that requires no change to the existing wiring networks. However, it has poor PQ parameters. By chopping the input voltage to dim the LED lamp, the nonlinear behavior of the LED as a load will inject undesirable harmonics into the network. Moreover, under rated conditions with zero firing angle the TRIAC switch will always be conducting which will

add to the conduction loss of the overall system even if no dimming is required. Another significance is that for a sudden change in the chopped input voltage, an inrush current will flow to charge up the input Electrolytic Capacitors (E-Caps). The drawn current by an LED driver will have a second-order system characteristics as follows,

$$I_D = \frac{V_{dc}}{L_f C_f} \frac{sC_f + \frac{1}{R}}{s^2 + s\frac{1}{RC_f} + \frac{1}{L_f C_f}} \quad (2)$$

$$V_{dc} = \frac{\sqrt{2}V_G}{\pi} (\cos\alpha + 1) \quad (3)$$

where R represents equivalent resistance of an LED string, V_{dc} the average DC voltage after rectifying the ac signal, and V_G is rms value of the grid voltage.

A high inrush current will lead to temperature rise of the E-Caps and hence complete failure [19]. This inrush current might damage the LED or shorten its lifetime.

C. Protocols of Dimming Systems

Low voltage dimming signal defined in IEC60929, in which the dimming signal is separated from the main supply voltage. It is applied mainly with external LED drivers. The low voltage signal can be analog (0-10V dimming protocol) as shown in Fig. 4 or Digital Addressable Lighting Interface (DALI) protocol as shown in Fig. 5. The dimming system consists of a switch that controls the turning on and off the LEDs and a low voltage dimming circuit. The communication is unidirectional in the analog system with no monitoring capability, while it is based on a bidirectional communication in the digital system. DALI protocol has a relatively yet acceptable low baud rate of 1.2 kbits per second (bps) [20]. The digital communication is done on a master-slave arrangement. Applying low voltage dimming protocol requires additional control wiring and proper LED driver controller that is compatible with the dimming protocol used. Low voltage dimming system provides central control in commercial and industrial buildings. It can be used with new installations other than replacing existing lighting system networks.

Smart bulbs and internet of things are gaining a lot of interest in the lighting industry. ZigBee and Z-wave are the most leading protocols that allow the user to wirelessly control the on/off, dimming, color change of the lighting sources. ZigBee operates at 2.4 GHz ISM band with 250 kbps data rate [21]. Z-wave does not interfere with Wi-Fi as it operates in 906 MHz in North America and 868 MHz in Europe [22]. Z-wave typically transmits information at data rate of 40 kbps. Both ZigBee and Z-wave are low power wireless communication protocol. They both employ mesh network topology where each device can connect to other devices (nodes) and find the nearest available path in the network within its range. A gateway node is needed to serve as a bridge between the mesh network and TCP/IP network as shown in Fig. 6. In contrast, Wi-Fi communication protocol [23], does not need a gateway for internet connectivity. The downsides of Wi-Fi technology is the high power consumption and high cost compared to other

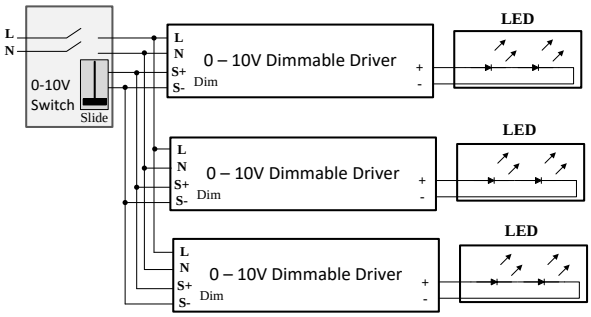

Fig. 4. 0-10V dimmer system.

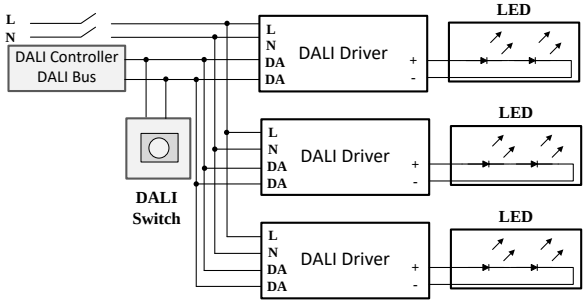

Fig. 5. DALI dimmer system.

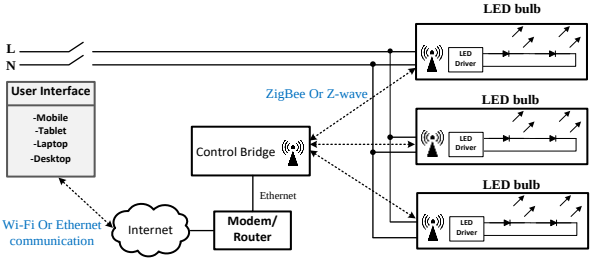

Fig. 6. Wireless dimmer system.

low power wireless protocols. Wi-Fi is based on a star network topology in which each node of the network is connected to the central node. A wireless control system based on ZigBee protocol has been proposed in [24]. The study has been conducted on a street lighting application with traffic based dimming strategy. The main drawback utilizing wireless smart dimming is that each LED driver has to support the wireless dimming protocol employed, e.g. Bluetooth, ZigBee, Zwave and Wi-Fi. This adds complexity to LED drivers and increases the cost of the network, especially for large penetrations of LEDs in streetlight or parking lot applications.

III. Proposed Remote Control Dimming System

The proposed system shown in Fig. 1 is a remote central dimming system for a large-scale LED lighting network. The system can attain continuous dimming for LED lamps while improving the PF and reducing the current harmonics that are generated by the internal driver, shown in Fig. 2, in commercial dimmable LEDs. The remote management system allows scheduling a continuous dimming profile for existing lighting systems, which will endorse energy saving. This can be accomplished by setting a profile to dim the LEDs

according to the ambient daylight or productivity requirement. Fig. 7 shows an example of a dimming profile for road lighting systems. For instance, the dimming level can be set to a high level in evening and early morning rush hours at which full energy is acquired. While, the dimming level can be set to decrease gradually during sunrise and to be zero during daylight. Furthermore, energy saving can be achieved during mid-night to set it as 80% brightness.

The system consists of three main parts: a VSC dimmer, a controller with a Wi-Fi module and a control center. The VSC dimmer controls the magnitude of the output voltage delivered to the LED lamps with a sinusoidal voltage. This will eliminate the inrush current drawn by the filter capacitor. By varying the output voltage magnitude, the LED driver will receive a new desired dimming level and change the output light intensity accordingly. The VSC dimmer controls the input current as well to achieve high PQ parameters at the input side. The controller receives the sensor signals and sends the PWM signals based on the desired reference signal. To build a remote management system, a Wi-Fi module is used to allow communication between the VSC dimmer, the controller, and the control center unit through internet. A desktop/webpage application running on a control center will be the interface between the operator and the VSC dimmer. The operator will send a command with a desired power to dim the LED lighting system. This information will be received by the Wi-Fi module, which will set the new operating point to the controller. The controller then will take the right action and send corresponding PWM signals to the VSC dimmer. The operator will be able to receive feedback information from the system for monitoring. Two feedback signals are sent: measured power in watts and LUX values.

IV. VSC Dimmer System Principle of Operation

Fig. 8 shows the VSC dimmer topology which consists of two half bridge VSCs that are connected to a common dc link capacitor. VSC1 is connected in parallel to the input voltage to mitigate all harmonics components absorbed by the load. While, VSC2 is connected in series between the input voltage and the LED lighting network to manage the voltage applied across the LEDs. The system control block diagram is shown in Fig. 8. The shunt VSC has two control loops; 1) outer control loop maintains the DC link capacitor at a constant value, 2) inner control loop shapes the input current (i_G) to be sinusoidal and in-phase to the grid voltage (v_G). The series VSC has one control loop to regulate the output voltage. The whole system achieves balance when the input power (p_G) equals the output power (p_O). Detailed control design and implementation can be found in [25], [26].

The proposed VSC dimmer can be modelled as a shunt voltage controlled current source and as a series voltage controlled voltage source as shown in Fig. 9. The apparatus achieves dimming by controlling the voltage applied to the lamps through the series voltage source. The dimmer operates

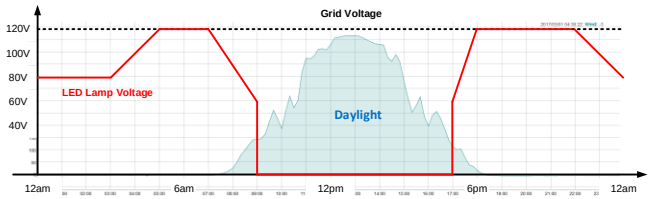

Fig. 7. Example of dimming profile for street lighting system.

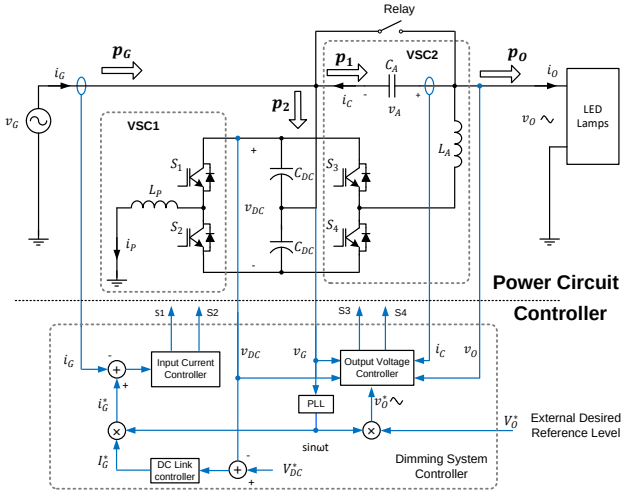

Fig. 8. Detailed VSC dimmer system topology and control block diagram.

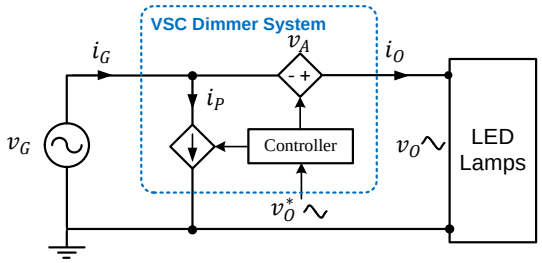

Fig. 9. Equivalent circuit of VSC dimmer system.

as a controllable voltage source v_A that is connected between the grid and the load voltage v_O. The voltage applied across the LEDs has a direct relationship with its output light intensity [10], from which the reference voltage that corresponds to a specific dimming level can be obtained. By varying the series voltage, a smaller voltage than the grid will be applied across the LEDs. This can be achieved using the following formula,

$$v_A^*(t) = v_o^*(t) - v_G(t) \tag{4}$$

where $v_A^*(t)$ is reference voltage-controlled voltage source, and $v_o^*(t)$ is the desired voltage applied to LED lamps.

Fig. 10 (a) shows the phasor diagrams under one dimming level. At steady state, the series voltage v_A is in out of phase of v_G delivering a smaller magnitude across the LEDs. The dc link voltage is regulated at a pre-set voltage level V_{DC}^*. By creating a power branch, the dimmer compensates and regulates the power delivery from the source to the load. The parallel converter will restore the power absorbed/delivered by the series converter as shown in Fig. 11 (a).

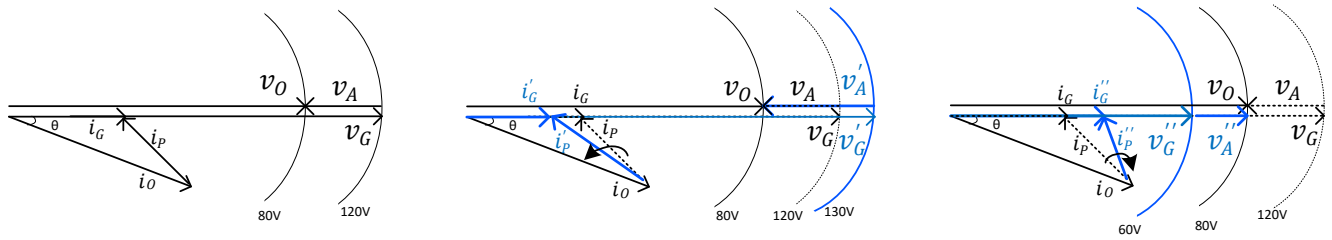

(a) (b) (c)

Fig. 10. Phasor diagrams of VSC dimmer system under a dimming level (a) steady state (b) voltage swell (c) voltage sag.

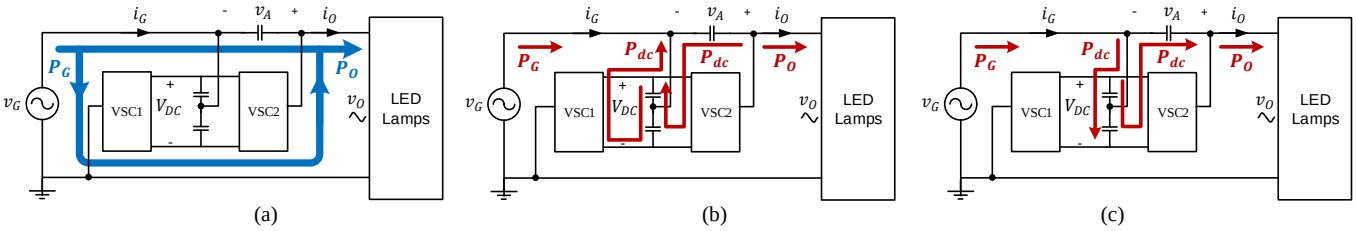

(a) (b) (c)

Fig. 11. Power flow under a dimming level (a) steady state (b) voltage swell (c) voltage sag.

Furthermore, the system is able to compensate a voltage sag/swell while maintaining the desired dimming level constant. In a voltage swell v'_G, the series voltage will increase v'_A maintaining v_O constant as illustrated in the phasor diagram in Fig. 10 (b). The parallel current i'_P will change accordingly to meet the new operating point after a change in i'_G. As the power delivered to the LEDs is maintained constant, the end user will experience no change in the output light intensity. During transient, the excess power will be absorbed by the dc link capacitor as shown in Fig. 11 (b). Contrary, in a voltage sag, v''_A will be in phase with v''_G as shown in Fig. 10 (c). The real power demand is supplied by the dc link capacitor during transient as depicted in Fig. 11 (c). The dc link capacitor will charge back up to steady state through the parallel VSC.

V. Remote System and Devices

A. Data Acquisition and Communication

The system is a bidirectional communication between the VSC dimmer and the control center unit. Data acquisition is done through the sensors and sampled with A/D converter in a digital signal processing (DSP). Fig. 12 shows the detailed system architecture between the VSC dimmer system, DSP, Wi-Fi module, and the control center. Voltage sensors are for input voltage, output voltage that is applied across the lighting network, dc capacitor voltage, and current sensors are for input current and filter capacitor current i_C. A developed control algorithm will define the switching actions according to the instantaneous sensed signals. At the same time, data transfer is taking place between the DSP and the Wi-Fi module through serial or parallel communication. UART, SPI, or GPIO can be used for interface. The Wi-Fi module is responsible to sending/receiving the data to/from the server. The control center that represents the remote management system will receive/send the data from/to the server.

B. User Interface Implementation

Graphical User Interface (GUI) is designed to allow the user to send commands and receive feedback information through a webpage or a desktop application. The user can send a request through the webpage browser. HTTP is used a communication protocol between the client and the host server. The Wi-Fi module runs a program (written in the Python programming language), which reads and writes data to the server. The user will set a desired reference value through the web browser. This external dimming signal will be sent to the VSC dimmer system. The Wi-Fi module will request this information and get a response from the web server. A command will be sent from the Wi-Fi module to the DSP to change the reference signal. For monitoring the system performance, the sensed signals at the load side are used to calculate the average power delivered. The server will request to display this information on the GUI. MATLAB software is used for the purpose of implementing a desktop application. The application running on the control center will communicate with the Wi-Fi module through Secure Shell (SSH) connection. The user will set a desired power level using the desktop application. As a response, the controller will take a proper control action according to the received new desired reference signal. The desktop application will always allow remote controlling to the dimmer system even if the internet connection is down through the LAN network, which will increase the overall system reliability. In addition, the operator will be able to monitor real-time light intensity values. This is achieved by placing a LUX meter at the lighting network side. The Wi-Fi module will receive the lux value through I2C pins or wirelessly using Zigbee.

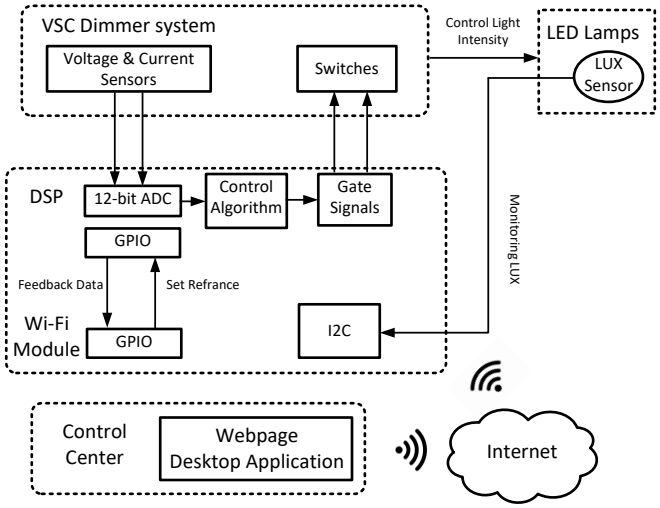

Fig. 12. System architecture of communication and interface.

VI. SYSTEM MODELLING AND CHARACTERIZATION

A. *Stability of Control system*

As discussed in section IV, the series converter is responsible for delivering a smaller voltage across the LEDs than the applied main supply voltage. There are two modes of S_3 and S_4, in which they are operating opposite to each other and independent from S_1 and S_2. The converter's state variable equations are represented by,

$$\frac{di_L}{dt} = \frac{1}{L_A}\left[\frac{v_{DC}}{2}(2d(t)-1) - v_A\right] \tag{5}$$

$$\frac{dv_A}{dt} = \frac{1}{C_A}\left(i_L - \frac{v_A+v_G}{R}\right) \tag{6}$$

where $d(t)$ is average of converter switching function $q(t)$. Derivation of (5) & (6) can be found in the appendix.

At steady state equilibrium point, the duty ratio *D* of the converter can be found. It will be a time varying quantity. Its value depends on the amount of the input voltage and the desired output voltage as a sinusoidal waveform,

$$D(t) = \frac{v_o(t)-v_G(t)}{v_{DC}} + \frac{1}{2} \tag{7}$$

The boundary control with a second-order switching surface has a fast dynamic response [27]. A small signal block diagram of the proposed control scheme is shown in Fig. 13. $T_{PS}(s)$ and $T_{BC}(s)$ represent the transfer function of the power stage and the controller respectively. The closed loop transfer function of the system $G_{BC}(s)$ is expressed as follows [28],

$$G_{BC}(S) = \frac{\tilde{v}_O(s)}{\tilde{v}^*{}_O(s)} = \frac{1}{\frac{T}{4}s+1} \tag{8}$$

where *T* is switching period.

The frequency response of the boundary control is shown in Fig. 14, in which the boundary control simplifies the system into a first order system that acts as a low pass filter with a bandwidth of 6.35 kHz. The system receives the reference from an external signal that is originated by the end user. This signal represents a desired dimming level. As the data will be transmitted over the internet, a network latency is introduced. Consequently, a system delay, t, is introduced in the control loop. A network latency is the time it takes for a data to travel from one point to another over the network. The transfer function of communication delay, represented by $T_{comm}(s)$, will not affect the stability of the system as it will be much slower than the voltage control loop. Therefore, it will not influence the performance of the overall system. The overall system transfer function of the system is expressed by,

$$T_{comm}(S) = \frac{\tilde{v}_O^*(s)}{\tilde{v}_{OR}^*(s)} = T_D(s).T_{ZOH} = e^{-t_1 s}.\frac{(1-e^{-t_2 s}s)}{t_2 s} \tag{9}$$

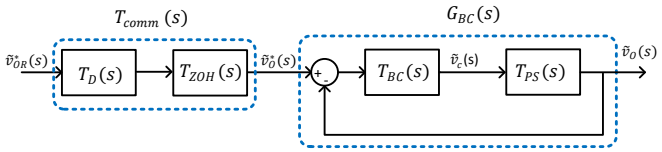

Fig. 13. Small signal model the VSC dimmer system control scheme.

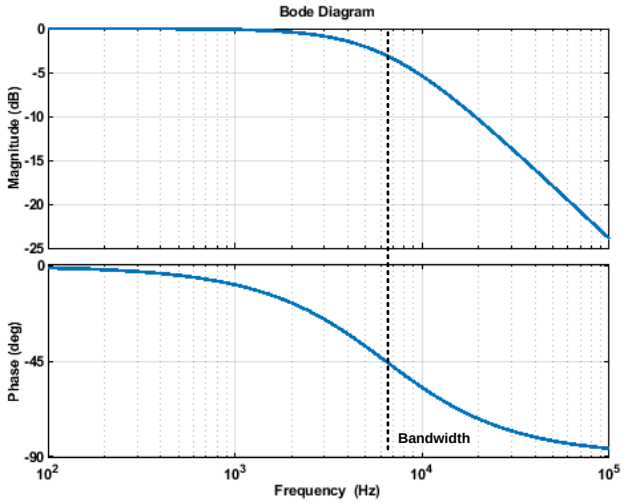

Fig. 14. Frequency plot of boundary control.

B. *System Loss Estimations*

Loss breakdown of the system has been estimated for system design optimization. The semiconductor devices and the filter inductors cause the main losses in the converter. In this study, the Trench Field Stop (FS) IGBTs have been selected due to their high performance and low conduction and switching losses. Semiconductor losses are estimated according to [29], in which the losses are determined using the electrical characteristics specified in the datasheet for the corresponding operating point. The magnetic material used to form the inductor is the Metglas C-Core AMCC. The inductor core loss are calculated based on "Steinmetz" equation as follows,

$$P_{croe} = 6.5.f^{1.51}.B_{ac}^{1.74}.wt \tag{10}$$

where, f is the switching frequency in kHz, B_{ac} is ac flux and wt is the weight of the core [30].

The behaviour of the LED as a load has been characterized

according to the data given in [10]. Fig. 15 shows the estimated loss in a 500VA/120V dimmer system. For a light load (e.g. small number of connected LEDs) the efficiency of the system is low, this is because the switching losses are dominant at low power levels. The conduction losses are increasing as the number of connected LEDs to the system increases. Fig. 16 shows that the efficiency will increase when a larger scale of lighting network is supplied.

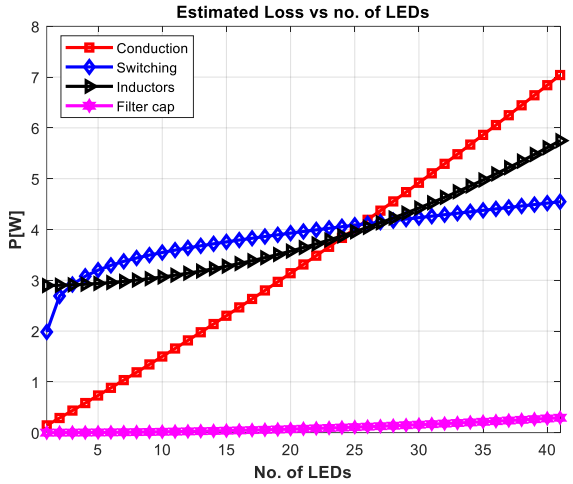

Fig. 15. Estimated loss in 500VA, 120V VSC dimmer system.

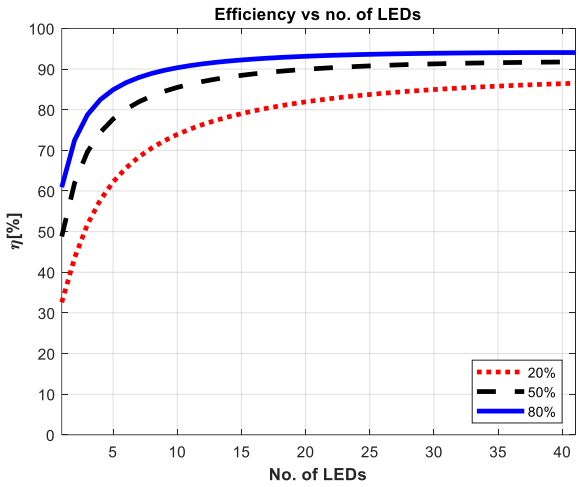

Fig. 16. Estimated Efficiency of 500VA/120V VSC dimmer system under various dimming levels, 20%, 50% and 80% of rated illuminance.

VII. EXPERIMENTAL VERIFICATIONS

A. *Implementation of Testbed*

A 500VA/120V, VSC dimmer prototype has been implemented to verify the proposed dimming system shown in Fig. 17. Fig. 18 shows the desktop control panel of the remote dimmer system. An ac power supply is used to provide input power to 9 dimmable LEDs, each of 12 W power consumption that is equivalent to 60 W incandescent lamp. A power analyzer is used to measure PQ parameters including PF, total harmonic distortion of output voltage (THD_{V_O}), total harmonic distortion of input current (THD_I), and efficiency (η).

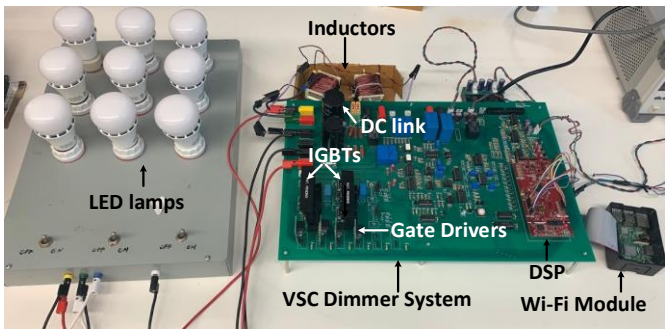

Fig. 17. Testbed setup.

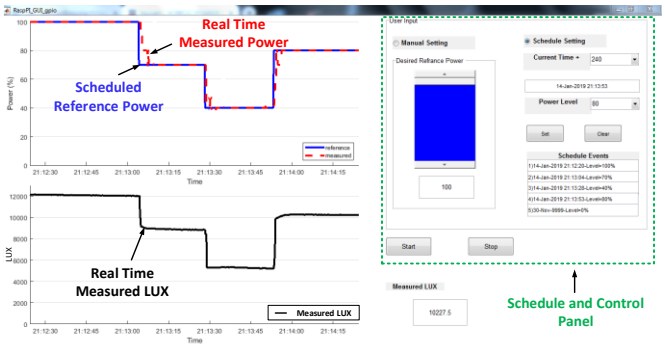

Fig. 18. Desktop application for dimming lighting systems.

B. *Evaluation of Dimming Performance*

In order to benchmark the performance, a standard TRIAC-based dimmer is used to provide dimming function for LED lamps. The results in Fig. 19 (a) show the waveforms of the input voltage, output voltage across LEDs, LED current and input current drawn at 50% light intensity. There's an inrush current when the TRIAC turns on to charge up the filter capacitor as discussed in eq. (2). The inrush current is found to be 10 times the magnitude of the LED rated current. This inrush current might shorten the life time of the LEDs and decreasing its luminous efficacy. Conversely, the VSC dimmer system has been utilized to provide dimming to the LEDs under test. Fig. 19 (b) shows the waveforms at 72 V RMS reference output voltage, which corresponds to 50% light intensity. The results show high quality waveforms for input current and output voltage as well as LED current.

C. *Static Power Quality Evaluations*

Power analysis measurements are shown in Fig. 20 to study the effect of different dimming levels on PQ parameters, including THD_I, THD_{V_O} (lamp voltage), PF, η, output/input power and input VA, utilizing TRIAC and VSC dimmers. The TRIAC dimmer failed to achieve 100% illuminance due to the very small firing angle for conducting all the time even though no dimming requirement ($\alpha \cong 0$). The graphs show that, with using TRIAC dimmer higher harmonic contents as well as lower PF are experienced when the lamps are dimmed. This is due to the higher delay angle at lower dimming levels. On the contrary, the VSC dimmer shows a better performance in terms of PQ parameters. Regardless of, the TRIAC dimmer has a

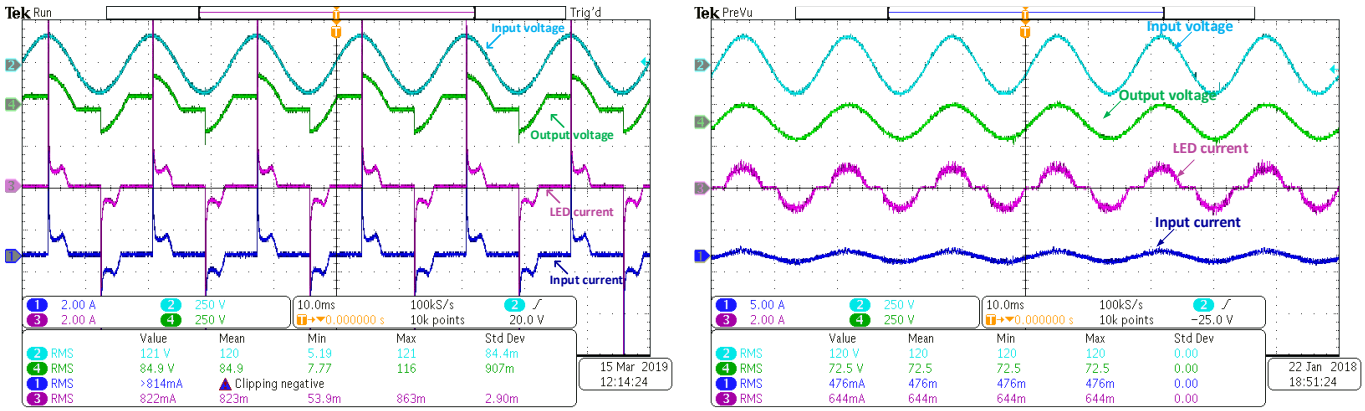

(a) (b)

Fig. 19. Waveforms at 50% illuminance with (a) TRIAC-based dimmer (b) VSC dimmer system.

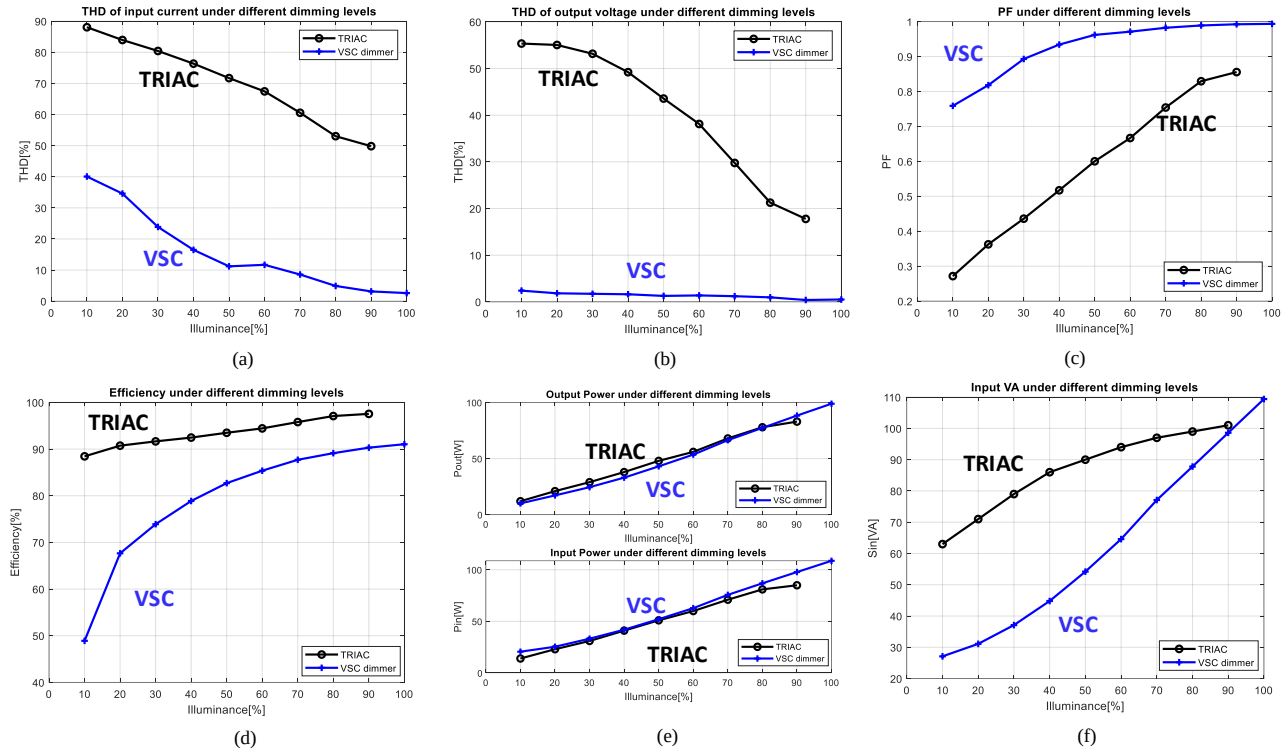

(a) (b) (c) (d) (e) (f)

Fig. 20. Power quality measurements comparison (a) THD of input current (b) THD of lamp voltage (c) PF (d) efficiency (e) output/input power (f) input VA.

high efficiency as in Fig. 20 (d); the output power drawn to achieve the same level of illuminance in LUX using a TRIAC dimmer is higher compared to that using the VSC dimmer system as shown in Fig. 20 (e). The reason is that the inrush current that will go into an LED, while using the TRIAC dimmer, will lead to an increase in the LED junction temperature. Higher LED junction temperature will lead to a lower luminous efficacy meaning lower lm/W [31]. Therefore, the input power drawn for both dimmer systems are quite similar. In addition, the input VA is much lower using the VSC dimmer due to its high PF in Fig. 20 (f). Thus, the VSC dimmer has an overall better performance compared to the traditional dimmer. It is also important to mention that there are 9 LEDs under this test according to the laboratory scale setup. This justifies the low measured efficiency at light load. Especially at 10% illuminance that corresponds to only 4% of the system full rating. This has been estimated and justified in section VI. B. The efficiency of the system can increase significantly when it is fully utilized or with the use of recent development of power semiconductor - wideband gap semiconductor devices.

D. Voltage Sag and voltage swell.

If a voltage sag/swell occurs in the network, the driver of a dimmable LED identifies it as a request of changing its light intensity. Therefore, the end user will observe visible flickering for the period of the sag/swell. The VSC dimmer system is able to compensate a voltage sag or swell in the network. A test has been conducted at 70% dimming level, in

TABLE I
COMMUNICATION PARMETERS.

Parameter	Value
t_1	5 ms
t_2	10 ms
I2C	9600 bps

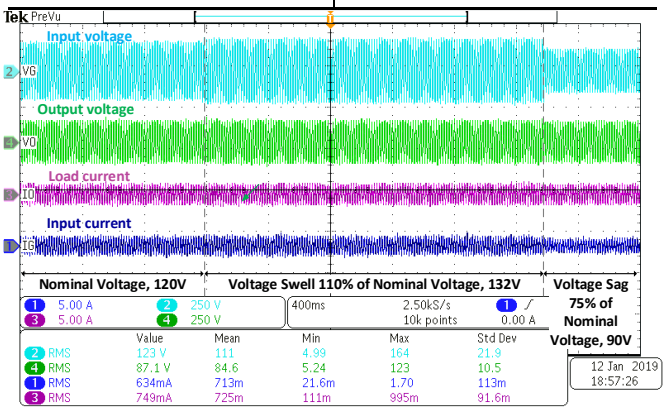

Fig. 21. 70% dimming level under voltage sag and voltage swell.

which the voltage across the LEDs has been controlled at 87 V rms. A voltage swell and then a voltage sag, 110% and 75% of the nominal grid voltage, respectively, have been applied to the main supply. The VSC dimmer system was able to maintain the output voltage constant in both transient conditions as shown in Fig. 21. Therefore, the power delivery has been maintained constant as well.

E. Interactive GUI and Network Latency

A snapshot of the webpage is presented in [1]. The GUI allows the user to set a dimming level either manually through a slider or automatically by setting a schedule to create a dimming profile for the day. It can be accessible anywhere using a laptop or a cell phone. The desktop application snapshot is shown in Fig. 18. The schedule event for the conducted test is to change the power level from 100% rated power to 70%, 40% then 80%. The results show that the real-time measured power and light intensity are following the change in the power level. The GUI displays the measured light intensity feedback signal using TSL25661 luminosity sensor.

The data transferring through the network can definitely introduce delay and inconsistency in time. The total network latency has been characterized running a MATLAB program. First, The MATLAB program initiates communication with the Wi-Fi module to send data and commands through the network before actual execution takes place. Likewise when transferring back data from the Wi-Fi module to MATLAB program. Table I gives the average travel time of the message in the network under the performed test conditions.

VIII. CONCLUSIONS

A comprehensive remote control dimming technique for commercial dimmable LED lamps has been proposed. The proposed system does not require rewiring the existing lighting network while providing remote dimming control function with high PQ features. The technique is based on adding a VSC dimmer system between the main supply and the LEDs. The VSC dimmer system achieves high PQ parameters compared to conventional diming techniques. Moreover, the system is able to compensate for voltage variations in the network resulting in a flickering free lighting network. The operator at the control center can control dimming through a webpage or a desktop application. The system employs a bidirectional communication between the VSC dimmer system and the control center. No specific additional controller for the LED driver is required. A 500 VA system has been prototyped and apparently evaluated. The results show good agreements with the theoretical concept. This technique is promising for street lighting or commercial lighting systems that require large penetration of LEDs with central dimming and monitoring.

REFERENCES

[1] R. M. Abdalaal, C. N. M. Ho, C. K. Leung, N. I. Ohin and S. H. Ur Rehman, "A Remotely Control Dimming System for LED Lamps with Power Factor Correction," *IEEE ECCE*, 2018, pp. 4721-4727.
[2] CEATI International Inc., "Lighting Energy Efficiency Reference Guide," 2014.
[3] LUXEON Rebel, “Reliability Data,” Reliability Datasheet RD07, Philips, Lumileds, 2007.
[4] S. Di Mauro, S. Musumeci, A. Raciti and G. Vasta, "Analysis of the current harmonics injected into the power grid by dimmable LED lamps," *AEIT*, 2016, pp. 1-6.
[5] Electromagnetic compatibility (EMC) – Part 3-2: Limits – Limits for harmonic current emissions (equipment input current ≤16 A per phase), IEC Standard 61000-3-2, 2001.
[6] J. Molina, J. J. Mesas, N. Mesbahi and L. Sainz, "LED lamp modelling for harmonic studies in distribution systems," *IET Gener., Transm. & Dist.*, vol. 11, no. 4, pp. 1063-1071, 9 3 2017.
[7] A. Wilkins, J. Veitch and B. Lehman, "LED lighting flicker and potential health concerns: IEEE standard PAR1789 update," *IEEE ECCE*, 2010, pp. 171-178.
[8] S. Li, Y. Guo, S. Tan and S. Y. R. Hui, "An Off-line Single-Inductor Multiple-Output LED Driver With High Dimming Precision and Full Dimming Range," *IEEE Trans. Power Electron.*, vol. 32, no. 6, pp. 4716-4727, 2017.
[9] M. Bodetto, A. E. Aroudi, A. Cid-Pastor and M. S. Al-Numay, "Improving the Dimming Performance of Low-Power Single-Stage AC–DC HBLED Drivers," *IEEE Trans. Ind. Electron.*, vol. 64, no. 7, pp. 5797-5806, 2017.
[10] R. M. Abdalaal and C. Ho, "Characterization of commercial LED lamps for power quality studies," *IEEE EPEC*, 2017, pp. 1-6.
[11] H. Chung, C. Ho and S. Hui, “Apparatus and method for providing dimming control of lamps and electrical lighting systems,” *UK Patent*, No. GB2405540, 10/05/2006.
[12] L. Lohaus, et al., “A Dimmable LED Driver with Resistive DAC Feedback Control for Adaptive Voltage Regulation,” *IEEE Trans. Ind. Appl.*, vol. 51, no. 4, pp. 3254–3262, 2015.
[13] W. L. D. Via, et al., “Color Variation Reduction of GaN-Based White Light-Emitting Diodes Via Peak-Wavelength Peak-Wavelength Stabilization,” *IEEE Trans. Power Electron.*, vol. 29, no. 7, pp. 3709–3719, 2014.
[14] L. Svilainis, "Comparison of the EMI Performance of LED PWM Dimming Techniques for LED Video Display Application," *J. Display Technol.*, vol. 8, no. 3, pp. 162-165, 2012.

[15] Q. Wang, T. Li and Q. He, "Dimmable and Cost-Effective DC Driving Technique for Flicker Mitigation in LED Lighting," *J. Display Technol.*, vol. 10, no. 9, pp. 766-774, 2014.
[16] W. Lun, K. H. Loo, S. Tan, Y. M. Lai and C. K. Tse, "Bilevel Current Driving Technique for LEDs," *IEEE Trans. Power Electron.*, vol. 24, no. 12, pp. 2920-2932, 2009.
[17] J. Okumura, Y. Kozawa, Y. Umeda and H. Habuchi, "Hybrid PWM/DPAM Dimming Control for Digital Color Shift Keying Using RGB-LED Array," *IEEE J. Sel. Areas Commun.*, vol. 36, no. 1, pp. 45-52, 2018.
[18] W. Ma, X. Xie, Y. Han, and H. Deng, "Control scheme for TRIAC dimming high PF single-stage LED driver with adaptive bleeder circuit and non-linear current reference," *IEEE APEC*, 2016, pp. 816–821.
[19] C. Shin, et al., "Sine-Reference Band (SRB)-Controlled Average Current Technique for Phase-Cut Dimmable AC–DC Buck LED Lighting Driver Without Electrolytic Capacitor," *IEEE Trans. Power Electron*., vol. 33, no. 8, pp. 6994-7009, 2018.
[20] R. Lenk and C. Lenk, *Practical Lighting Design with LEDs*, Wiley-IEEE Press, 2011.
[21] J. Wang, "Zigbee light link and its applications," *IEEE Wireless Commun*., vol. 20, no. 4, pp. 6-7, 2013.
[22] M. Knight, "Wireless security - How safe is Z-wave?," *Comput. & Control Eng. J*., vol. 17, no. 6, pp. 18-23, 2006.
[23] M. Zhiguo and W. Haiyan, "Design of LED light parameters controlled based on WiFi," *SSLChina: IFWS*, 2017, pp. 48-51.
[24] G. Shahzad, H. Yang, A. W. Ahmad and C. Lee, "Energy-Efficient Intelligent Street Lighting System Using Traffic-Adaptive Control," *IEEE Sensors J*., vol. 16, no. 13, pp. 5397-5405, 2016.
[25] R. M. Abdalaal and C. N. M. Ho, "Transformerless single-phase UPQC for large scale LED lighting networks," *IECON, 2017*, pp. 1629-1634.
[26] V. S. Cheung, et al., "A Transformer-Less Unified Power Quality Conditioner with Fast Dynamic Control," *IEEE Trans. Power Electron*., vol. 33, no. 5, pp. 3926-3937, 2018.
[27] C. N. Ho, H. S. H. Chung and K. T. K. Au, "Design and Implementation of a Fast Dynamic Control Scheme for Capacitor-Supported Dynamic Voltage Restorers," *IEEE Trans. Power Electron*., vol. 23, no. 1, pp. 237-251, Jan. 2008.
[28] Y. He, H. S. Chung, C. N. Ho and W. Wu, "Use of Boundary Control With Second-Order Switching Surface to Reduce the System Order for Deadbeat Controller in Grid-Connected Inverter," *IEEE Trans. Power Electron.*, vol. 31, no. 3, pp. 2638-2653, March 2016.
[29] C. N.M. Ho, H. Breuninger, S. Pettersson, G. Escobar, L. A. Serpa, and A. Coccia, "Practical design and implementation procedure of an interleaved boost converter using SiC diodes for PV applications," *IEEE Trans. Power Electron.*, vol. 27, no. 6, pp. 2835–2845, Jun. 2012.
[30] "Power factor correction inductor design for switched mode power supplies using Metglas Powerlite C-Cores," Metglas Application Guides.
[31] M. E. Raypah, B. K. Sodipo, M. Devarajan and F. Sulaiman, "Estimation of Luminous Flux and Luminous Efficacy of Low-Power SMD LED as a Function of Injection Current and Ambient Temperature," *IEEE Trans. Electron Devices*, vol. 63, no. 7, pp. 2790-2795, 2016.

APPENDIX

A. Derivation of (5) and (6)

The state space variables of the series VSC is expressed as,

$$x(t) = \begin{bmatrix} i_L \\ v_A \end{bmatrix} \ , u(t) = \begin{bmatrix} v_{dc} \\ v_G \end{bmatrix}, y(t) = v_A \tag{A.1}$$

During the switching period DT, the dynamic behaviour of the inductor current and the capacitor voltage can be found as,

$$\frac{di_L}{dt} = \frac{1}{L_A}\left(\frac{v_{DC}}{2} - v_A\right) \tag{A.2}$$

$$\frac{dv_A}{dt} = \frac{1}{C_A}\left(i_L - \frac{v_G + v_A}{R}\right) \tag{A.3}$$

While, during the switching period $(1 - D)T$

$$\frac{di_L}{dt} = \frac{1}{L_A}\left(\frac{-v_{DC}}{2} - v_A\right) \tag{A.4}$$

$$\frac{dv_A}{dt} = \frac{1}{C_A}\left(i_L - \frac{v_G + v_A}{R}\right) \tag{A.5}$$

By defining a switching function $q(t)$, (5) and (6) can be derived,

$$q(t) = \begin{cases} 1 & S_3\ ON, S_4\ OFF \\ 0 & S_3\ OFF, S_4\ ON \end{cases} \tag{A.6}$$